Phase Evolution, Densification And Dielectric Properties Of $[KNbO_3]_{1-x}[BaNi_{½}Nb_{½}O_{3-\delta}]_x[x=0.1,0.2]$ Ferroelectric Ceramics Prepared By Conventional Sintering And Spark Plasma Sintering

A

THESIS SUBMITTED IN PARTIAL FULFILLMENT

OF THE REQUIREMENTS FOR THE DEGREE OF

MASTER OF TECHNOLOGY (DUAL DEGREE)

in

INDUSTRIAL CERAMICS

By

Dhirendra Kumar Patro

Under the Guidance of

Prof. Ranabrata Mazumder

Department of Ceramic Engineering

National Institute of Technology

Rourkela – 769 008

DEPART MENT OF CERAMIC ENGINEE RING

NATION AL INSTI TUTE OF T ECHNOL OGY,

ROURKELA-769008

CERTIFICATE

This is to certify that the thesis on "**Phase Evolution, Densification and Dielectric Properties of $[KNbO_3]_{1-x}[BaNi_{½}Nb_{½}O_{3-\delta}]_x$ [x=0.1,0.2] Ferroelectric Ceramics Prepared By Conventional Sintering and Spark Plasma Sintering**" submitted by **Mr. Dhirendra Kumar Patro,** to the National Institute of Technology, Rourkela in partial fulfillment of the requirements for the award of the degree of **Master of Technology (Dual degree) in Industrial Ceramics** is a record of bonafide research work carried out by him under my supervision and guidance. His thesis, in my opinion, is worthy of consideration for the award of degree of Master of Technology in accordance with the regulations of the institute.

The results embodied in this thesis have not been submitted to any other university or institute for the award of a Degree.

Mr. S. Chakraborty
Co-Supervisor
CSIR-CGCRI
Kolkata

Prof Ranabrata Mazumder
Supervisor
National Institute of Technology
Rourkela

Acknowledgement

It is with a feeling of great pleasure that I would like to express my most sincere heartfelt gratitude to Prof. Ranabrata Mazumder**,** Dept. of Ceramic Engineering, NIT, and Rourkela for suggesting the topic for my thesis and for his ready and able guidance throughout the course of my preparing the report. I thank you, Sir, for your help, inspiration and blessings.

Special thanks to Mr. S. Chakraborty, CSIR-CGCRI for his advice and support and allowing me to work in CSIR-CGCRI under his guidance. I am thankful to Dr. Probal K. Das, Head Non-oxide ceramics and Composite division, CSIR-CGCRI for his kind support and providing the necessary facility. I am also thankful to Mr. Kamal Dasgupta, Director, CSIR-CGCRI for giving permission for joint M.Tech (Dual degree) project work. I am grateful to Mr. Awadesh Kumar Mallick of CSIR-CGCRI for the help in Raman Spectroscopy measurements. I express my sincere thanks to Prof. S.K. Pratihar, Head of the Department of Ceramic Engineering, NIT, Rourkela for providing me the necessary facilities in the department.

I would also take this opportunity to express my gratitude and sincere thanks to my honorable teachers Prof. S. Bhattacharyya and Prof. S.K.Pal for their invaluable advice, constant help, and encouragement.

I would like to thank my parents and other family members for their support for choices in all my life and their love, which has been a constant source of strength for everything I do. Also, I thank all my friends who had been had helped and supported me all throughout the year for the completion of my thesis.

I would also express my sincere thanks to laboratory Members of Department of Ceramic Engineering, N.I.T. Rourkela.

DHIRENDRA KUMAR PATRO

ROLL NO: 710CR1173

Abstract

Ferroelectric semiconducting ceramics with band gap (Eg)< 2 eV will be very useful for photovoltaic and photocatalytic application. Unfortunately all the current ferroelectric oxides have wide band gaps (Eg>2.7 eV for BiFeO3, Eg>3.5 eV for PZT) and can utilize only about 8%–20% of the solar spectrum and efficiency is very small. Recently, Grinberg et al. [US patent 2013/0104969, Nature 503 (2013) 509] invented a complex ceramic solid solution of $KNbO_3$-$BaNiNbO_3$ (KN-BNNO) which is ferroelectric and band gap < 2 eV. However, the problems associated with the development of the $KNbO_3$-based materials lies on its complex densification behavior and alkali evaporation leading to poor density. There is no literature available for the preparation of highly dense KN-BNNO ceramics by SPS sintering and study of it's dielectric property.

Present thesis reports the preparation of (1-x)$KNbO_3$-x$BaNiNbO_3$ powder by solid state synthesis route. Phase evolution with composition modification and calcination temperature was discussed. Dense (1-x)$KNbO_3$-x$BaNiNbO_3$ (x=0.1, 0.2) ceramics were prepared by a novel spark plasma sintering (SPS) technique. The sintering was conducted at temperatures ranging from 800 to 1075^oC under 35 MPa pressure. A bulk density value up to 97% of true density was achieved in the process. This contrast to around 83% of the theoretical density achieved by conventional sintering at around 1120^oC. The dielectric properties also improved (with respect to conventionally sintered sample) for spark plasma sintered samples.

Contents

List of Figures		
		Page No.
1.1	Interrelationship of piezoelectric and its subgroups based on the symmetry.	3
1.2	Tetragonal ferroelectric distortion of the perovskite structure, illustrating two polarization states	4
1.3	Idealized permittivity of a ferroelectric material as a function of temperature.	5
1.4	The solar spectrum and E_g values of different materials after Grinberg et al.	8
1.5	Schematic showing the physical mechanism of the photovoltaic effect in a ferroelectric	9
2.1	$(KNbO_3)_8$–$(BaNb_{1/2}Ni_{1/2}O_{2.75})_4$ crystal structures K and Ba are shown by blue and green spheres, respectively; Nb–O_6 and Ni–O_6 are shown as brown and grey octahedral with O atoms at the vertices.	12
2.2	Material transfer path during sintering	16
2.3	Pulsed current flow through powder particles	16
3.1	Flow chart of the total experimental procedure followed in the synthesis of KBNNO pellets.	21
3.2	The schematic diagram for the spark plasma sintering process.	24
3.3	Phase diagram between current and voltage.	27
4.1	DSC-TG curve for KBNNO uncalcined powder after 12hrs milling.	29
4.2	XRD patterns of the (1-x) KN- x BNNO powder with x = 0, 0.05 ,0.1, 0.2	30
4.3	Raman spectroscopy of different composition KBNNO powders	31
4.4	The powder morphology of the double calcined powder	32
4.5	Dilatometry of the KBNNO-0.1 calcined sample	33
4.6	bulk density and volume shrinkage of the KBNNO-0.1 with respect to sintering temperature	34
4.7	Microstructures of (a) surface and (b) fracture of the conventionally sintered sample sintered 1120/2hrs	35
4.8	TG plot of unannealed SPS1050 sample	36
4.9	(a)Surface FESEM image and (b) and (c) showing mapping of potassium and	37

Chapter-1

INTRODUCTION

1. INTRODUCTION

Ferroelectricity is the property of certain non-conducting crystals, or dielectrics, that show spontaneous electric polarization (separation of the positive and negative electric charge, making one side of the crystal positive and the other negative) which can be reversed in direction on application of an appropriate electric field.

A distinct atom or ion in a dielectric is not exposed directly to an applied electric field but to a local field which contains a very different value. And under certain conditions, lattice polarization generates a local field which tries to stabilize the polarization further – a feedback mechanism. This indicates to the chance of "spontaneous polarization", which means lattice polarization in the absence of an external applied field. Such materials do exist and the "ferroelectrics" constitute an essential class among them [1].

To understand the definition of ferroelectricity, it is necessary to mention piezoelectricity and pyroelectricity because they have interesting relationship in terms of crystal structures. Crystals are classified into 32 point groups based on their symmetry. These point groups are divided into two classes which include a center of symmetry and without center of symmetry. There are 21 non-centrosymmetric point groups, 20 (except point group 432) of which exhibit piezoelectricity. Fig. 1.1 shows that there are 10 crystal classes out of a possible 20 that are designated as pyroelectric. Unlike the more general piezoelectric classes that produce a polarization under stress, the pyroelectrics develop this polarization spontaneously and form permanent dipoles in the structure. This polarization also changes with temperature hence, the term pyroelectricity. A subgroup of the spontaneously polarized pyroelectrics is a very special category of materials known as ferroelectrics. Ferroelectric materials have four subcategories: the perovskite (ABO_3) group, the pyrochlore group ($A_2B_2O_7$), the tungsten-bronze group (AB_2O_6), the bismuth layer structure group ($A_4B_3O_{12}$), among which the perovskite group is the most important and thus the most widely studied. The ABO_3 type

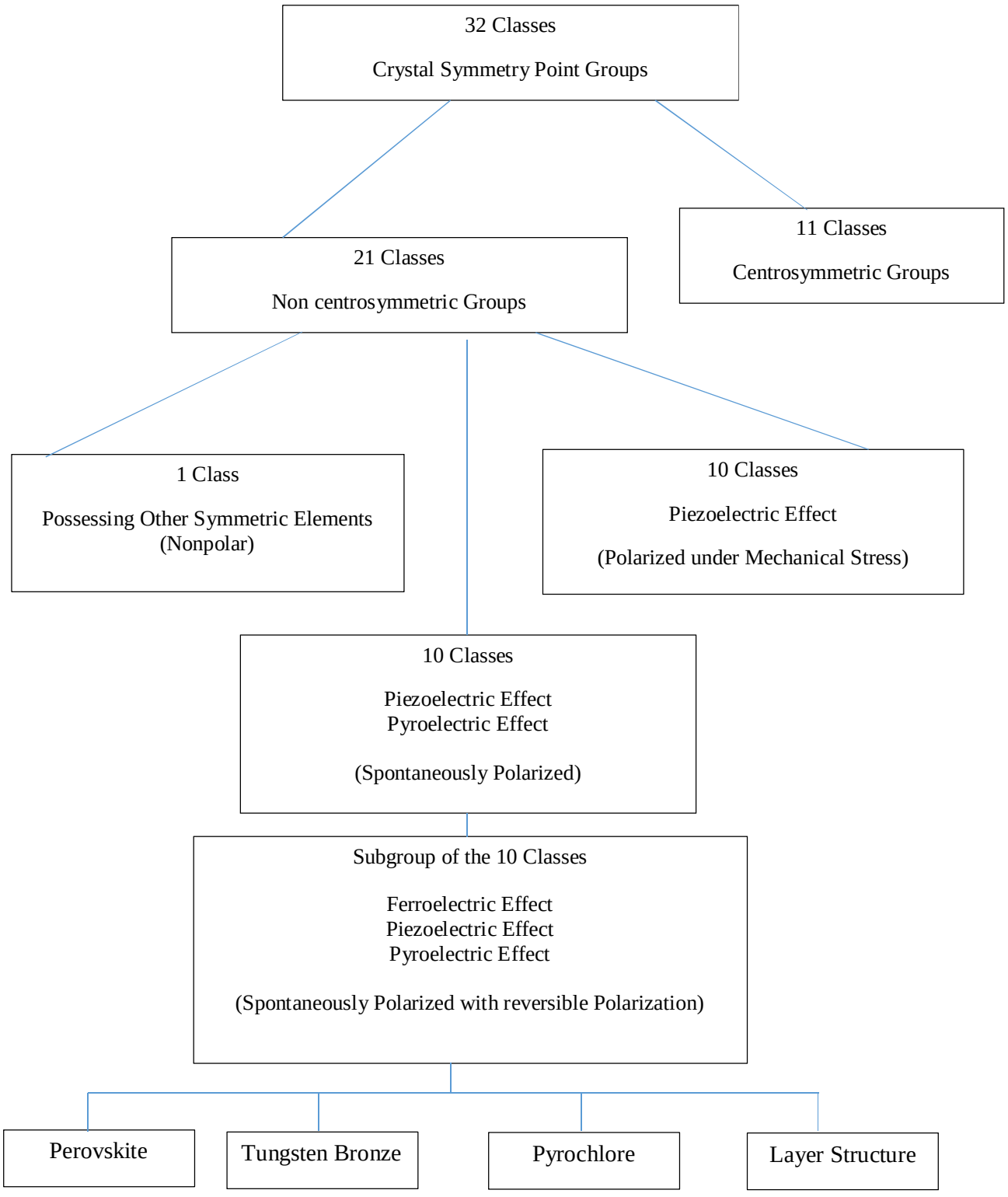

Fig. 1.1: Interrelationship of piezoelectric and its subgroups based on the symmetry.

ferroelectric ceramics are further divided into $BaTiO_3$, $Pb(Zr_xTi_{1-x})O_3$, $(Bi_{0.5}Na_{0.5})TiO_3$ and $KNbO_3$ family of compositions [2].

1.1 PEROVSKITE STRUCTURE

The mineral perovskite refers to Calcium Titanate, which has a chemical formula $CaTiO_3$. The majority of the commercially vital ferroelectric materials are found to have a perovskite like crystal structure. The perovskite oxides has a compositional formula of ABO_3, where A is in 12 fold coordination and B is in octahedral coordination with oxygen. (Fig 1.2). The A site remains at the corner of the cube, the B site stays at the center, and oxygen goes at every face center. The valance of the cation A can be +1, +2, +3 and cation B can be +4, +5, +6.

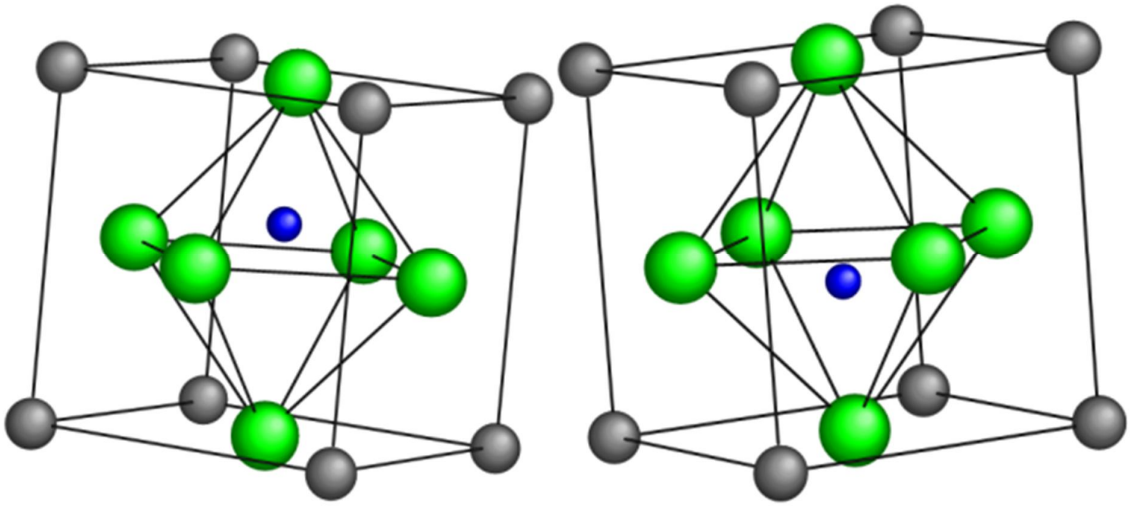

Fig. 1.2: Tetragonal ferroelectric distortion of the perovskite crystal structure, showing the two polarization states.

1.2 CHARACTERISTICS OF FERROELECTRIC MATERIALS

1.2.1. Curie Temperature

At a specific temperature, about every ferroelectric material go through a ferroelectric to paraelectric phase transition (in a few samples materials decompose before going into the paraelectric state) [1]. The temperature at which a ferroelectric material returns to the high temperature paraelectric stage is known as the Curie temperature (T_C). On cooling through T_C into a ferroelectric stage, a reorientable spontaneous polarization is created.

In ferroelectrics dominated by a displacive phase transition, for example, perovskite materials, the temperature dependence of the permittivity vary for 1st and 2nd order phase transitions. Fig. 1.3 shows the temperature dependence of the permittivity for displacive ferroelectric materials showing first or second order phase transitions.

2nd order phase transitions, which are normal for rhombohedral compositions, are usually characterized by a broad peak in permittivity. Ferroelectrics experiencing 1st order phase transitions, typical of tetragonal perovskite materials, however demonstrate a flat permittivity with increasing temperature straight up to the Tc.

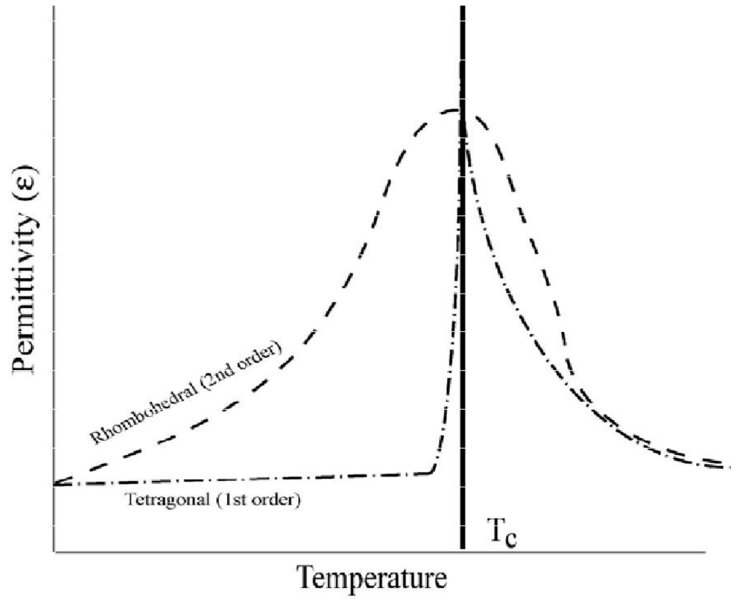

Fig. 1.3: Idealized permittivity of a ferroelectric material as a function of temperature.

1.3. IMPORTANT NARROW BAND GAP SEMICONDUCTING FERROELECTRICS

Ferroelectrics have recently attracted increased attention as a candidate class of materials for use in photovoltaic and other multifunctional devices. [3,4] However, one of the major obstacles that limit the photovoltaic application of ferroelectrics is their wide band gap (E_g). Since most of ferroelectrics have wide band gaps of above 3.0 eV, absorbing light in the Ultra-violet wavelength range. It was found that only multiferroic $BiFeO_3$ (BFO) has the lowest known band gap (2.7 eV) for a ferroelectric oxide [4]. BFO is capable of absorbing only 20% of the solar spectrum due to much larger E_g than optimal for photovoltaics. Researchers are identifying approaches to reducing the band gap of ferroelectrics without losing the useful ferroelectricity in complex metal oxides which may bring significant scientific and technological breakthroughs.

$KBiFe_2O_5$

Zhang et al. found a high curie temperature(T_C), smaller band gap (1.6 eV), very weakly ferroelectric and ferromagnetic compound, $KBiFe_2O_5$, from the tetrahedrally coordinated $A_2B_2O_5$ crystal structural family, having numerous traits suitable for the solar energy applications. It is the first to prove that inherently polar compounds made of transition metal MO_4 tetrahedral crystal system structures can offer much smaller band gaps than the traditional ferroelectrics ceramics, in this way a higher light absorption and a higher carrier concentration facilitates larger solar energy conversion.[5]

$LaCoO_3$-alloyed $Bi_4Ti_3O_{12}$

Choi et al presented an experimental as well as a theoretical study on ($LaCoO_3$)LCO-alloyed $Bi_4Ti_3O_{12}$ (BiT) (BiT–LC) to explain the possibility of the bandgap tuning in complex transitional metal oxides(TMOs). Through a site-specific substitutional alloying, they effectively reduced the bandgap as less as ~1 eV, without deteriorating the ferroelectric property of BiT. Moreover, they

observed enhanced photo-responses from alloyed BiT thin films, which confirmed the bandgap reduction. [6]

$Bi_7Fe_3Ti_3O_{21}$

Li et al. developed a simple method for preparing single-phase $Bi_7Fe_3Ti_3O_{21}$ nanoshelves. The $Bi_7Fe_3Ti_3O_{21}$ nanomaterial has a band gap of 2.22 eV with co-existing ferromagnetic and ferroelectric properties. $Bi_7Fe_3Ti_3O_{21}$ has an aurivillius structure. Layered Aurivillius phase materials has a general formula of $(Bi_2O_2)(A_{m-1}B_mO_{3m+1})$ and having the crystalline structure which is an repetition of perovskite-like layers with a composition of $(A_{m-1}B_mO_{3m+1})^{2-}$ and the fluorite-like layers of $(Bi_2O_2)^{2+}$. The properties of these type of layered Aurivillius ferroelectric materials could be widely controlled using versatile dopants and also by changing the layer number, m.[7]

$[KNbO_3]_{1-x}[Ba\ Ni_{½}\ Nb_{½}\ O_{3-\delta}]_x$ (KBNNO)

In 1951, Matthias and Remeika [8]discovered ferroelectricity in $KNbO_3$ (KN) reporting both its Curie temperature (T_C =435°C) and a second transition temperature at around 225°C. Further investigations revealed a sequence of phase transformations similar to those observed in $BaTiO_3$ [9].

$$\text{Rhombohedral} \xrightarrow{-10°C} \text{orthorhombic} \xrightarrow{220°C} \text{tetragonal} \xrightarrow{420°C} \text{cubic}$$

Pure $KNbO_3$ ceramics are difficult to fabricate, however, single crystals have been produced and interesting nonlinear electro-optic properties and piezoelectric coefficients along certain crystallographic directions have been reported. High coupling coefficients (k_T =0.69) and excellent temperature stability up to 160°C make $KNbO_3$ single crystals attractive for ultrasonic and acoustic wave transducer applications, however, other uses of $KNbO_3$'s piezoelectric properties are limited[1].

Recently Grinberg et al [10] was used the classic ferroelectric perovskite $KNbO_3$ (KN) to modify off-centre distortions and polarization and it was mixed with $BaNi_{1/2}Nb_{1/2}O_{3-\delta}$ (BNNO) to present a blend of Ni^{2+} on the B-site and an oxygen vacancy, which then can give rise to the electronic states

in the band gap of the KNO material. Fig 1.4 shows the band gap position of the KN and KN-BNNO in solar spectrum. The KN-based composition reported to have low band gap which can efficiently absorb in visible light range.

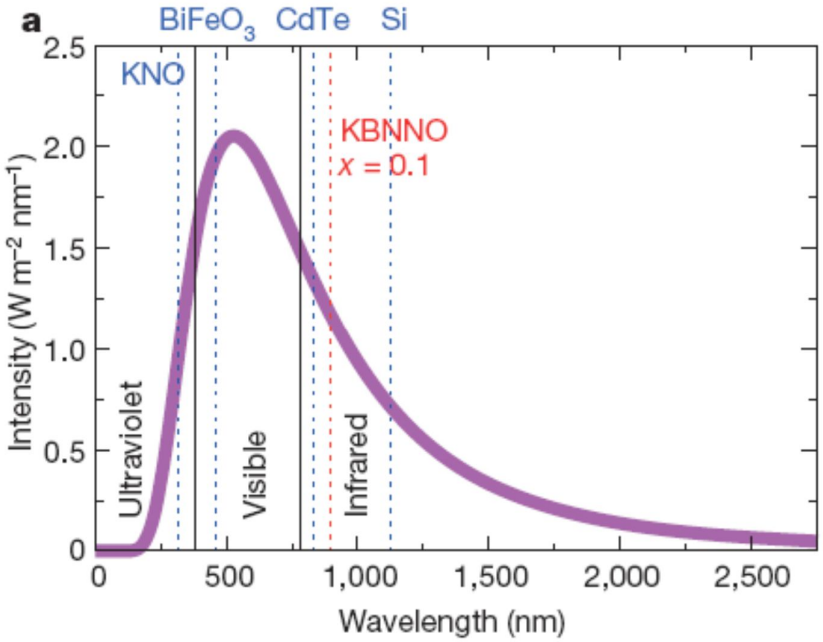

Fig.1.4: The solar spectrum and E_g values of different materials after Grinberg et al. [10]

1.4. APPLICATION OF SEMICONDUCTING FERROELECTRICS

In solar cells

Semiconducting ferroelectrics are best suitable for solar power generation because effect in semiconducting ferroelectrics is essentially a sort of a bulk-based effect, which differs from that of the conventional junction-based interfacial photovoltaic effect in the elemental semiconductors, such as the p-n junction or the Schottky junction. It has been as of late seen that there is an internal electric field in ferroelectric thin films all throughout the bulk region which starts from the electric polarization which is not totally counterbalanced by the screening charges. There are two mechanisms in charge of the photovoltaic effect in metal/Ferroelectric/metal structures. At the point when the light of a particular wavelength relating to the energy band gap of a material is incident on

an electrically poled ferroelectric, the photons are absorbed by the ferroelectric generating charge carriers which are the electrons and the holes. These photo-generated electrons and holes are then driven by the polarization induced internal electric field in the opposite directions toward the cathode and the anode, respectively, and in this way add to the photo-voltaic output. Subsequently, photovoltaic effect in the ferroelectric ceramics is basically a kind of a bulk-based effect, which contrasts from the ordinary junction based interfacial photovoltaic effect in the semiconductors, for example, p-n junctions or Schottky junctions. In the junction based semiconductors, open circuit photovoltage can't surpass the energy barrier height of the junction, which is generally lower than 1 V. Conversely, in the semiconducting ferroelectrics bulk photovoltaic effect, the remnant polarization and the polarization-induced internal electric field exist over the complete bulk region of the thin ferroelectric film instead of a thinner interfacial layer, as demonstrated in Fig 1.5 below, So in case of this the charge transportation is not restricted by diffusion, and the output photovoltage is not constrained by any energy barrier as that of normal junction based semiconductors..

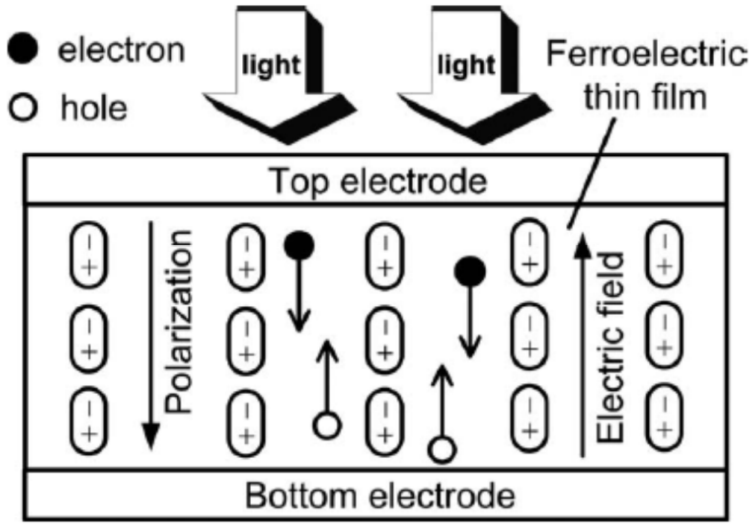

Fig. 1.5: Schematic showing the physical mechanism of the photovoltaic effect in a ferroelectric

Photocatalyst

Photocatalysts based on transition metal oxides working under UV-irradiation have been extensively investigated. However, considering the abundance of sun-light in the visible region (accounting for about 43% of incoming solar energy), the development of visible-light-photocatalysts is in demand for efficient utilization of solar energy.

In recent years, there has been tremendous research thrust in harvesting solar energy by visible-light-driven photocatalysis utilizing single-phase bulk and nanostructured metal oxides. [12] Ferroelectric semiconductor will be very useful due to their narrow bandgap.

Chapter-2

LITERATURE REVIEW

2.1. SYNTHESIS, Ddensification AND PROPERTIES OF $KNBO_3$-BASED COMPOUNDS

2.1.1. Solid state synthesis route

$[KNbO_3]_{1-x}[Ba\ Ni_{½}\ Nb_{½}\ O_{3-\delta}\ ]_x$ (KBNNO)

Grinberg et al[10] produced a clan of single-phase solid solutions made from cheaper and non-toxic elements using conventional solid-state synthesis methods:

This KBNNO is a semiconducting ferroelectric,which shows ferroelectric behavior and also has a wide variation in band gap on varying the composition. $KNbO_3$ was used as a parent material to deliver off centre distortion and polarization. To generate electronic states in the gap of the parent $KNbO_3$ material, so as to decrease its band gap, a blend of Ni^{2+} on the B site and an oxygen vacancy was introduced by mixing KNO with $BaNi_{1/2}Nb_{1/2}O_{3-\delta}$ (BNNO. The larger sizes of K and Ba cations support solubility and vacancy formation. Two of the twelve Nb^{5+} ions are replaced by Ni^{2+}, and four of the twelve K ions are replaced by Ba. This substitution generates an oxygen vacancy $V_O^{\cdot\cdot}$ adjacent to Ni_{Nb}'' defects (in Kroger–Vink notation) with the local dipole ($Ni–V_O$) parallel to the overall polarization. They obtained two stable KBNNO configurations, with the local structure of $Ni^{2+}–V_O–Ni^{2+}$ and $Ni^{2+}–V_O–Nb^{5+}$(Fig 2.1).The solid solutions $[KNbO_3]_{1-x}[Ba\ Ni_{½}\ Nb_{½}\ O_{3-\delta}\ ]_x$ (KBNNO). x = 0.1 – 0.5 were synthesized. They used cold isostatic pressing for green pellet preparation. The samples got sintered upto 95% of density.

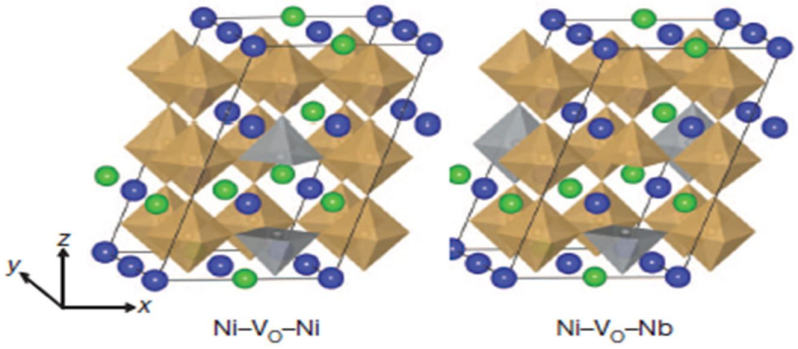

Fig. 2.1: $(KNbO_3)_8–(BaNb_{1/2}Ni_{1/2}O_{2.75})_4$ crystal structures K and Ba are shown by blue and green spheres, respectively; $Nb–O_6$ and $Ni–O_6$ are shown as brown and grey octahedra with O atoms at the vertices.[10]

They have reported this material to have very low band gap. But not much information about the phase formation, densification, sintering behaviour and dielectric properties of this material was provided.

Zhou at al. [12] studied the effects of BNNO doping on the structure, optical, and magnetic properties of KN powders, KN-xBNNO, x=0-0.3. They studied all the properties on powder sample. Powders of different composition were prepared by solid state method. The powder mixtures were presintered first at 1023 K, then uniaxially pressed into pellets and finally calcined at the optimum temperature range 1273–1473K for the different compositions. They found from XRD results, KBNNO crystals undergo structural transitions from orthorhombic to cubic phase with increasing x from 0 to 0.3. They found that the local crystal symmetry of KBNNO-0.1 compositions to deviate from the idealized cubic perovskite structure, which indicates both the occurrence of short-range distortions and the damping of the long-range ferroelectric order. Raman spectroscopy analysis shows that the structural phase transition mainly stems from the Ni2þ doping-induced local lattice strain. Additionally, they found that the band gap and magnetism of KBNNO can also be controlled by the BNNO doping content to obtain a narrow band gap multiferroic.

$KNbO_3$ based powder also can be prepared by other methods.

2.1.2. Hydrothermal Synthesis

For synthesis of $KNbO_3$ through hydrothermal route Nb_2O_5 is reacted with a KOH solution at 150 °C for 6–7 days.. Optimum concentration of KOH is important for the synthesis of $KNbO_3$ nano rods and nanowires. Low concentration of KOH will result in formation of KNb_3O_8 and $K_4Nb_6O_{17}$. and a very high KOH concentration will lead to “nano-fingers” consisting of stacked cube-shaped particles of different sizes. So an optimum concentration of KOH is necessary to form 1D nanostructures under these conditions. The formation of nano-fingers with non-uniform widths was attributed to defect accumulation, which created obstacle for further sidewise growth of the cubes into nanowires with uniform width.

2.1.3. Molten Salt Synthesis

Cheng et al [13,14] presented a molten salt technique to synthesize high-quality one-dimensional (1-D) K,Na NbO_3 (KNN) nanorods (NRs) with well-regulated K/Na ratios, For the molten-salt reaction, the key point is to obtain high-aspect-ratio Nb_2O_5 NRs,which then act as the templates for the formation of KNN NRs. First of all, the equiaxed Nb_2O_5 particles are transformed to high-aspect ratio NRs with the composition of $K_6Nb_{10.8}O_{30}$. The amount of K_2CO_3 influences the product morphology of the $K_6Nb_{10.8}O_{30}$ synthesized in first step. which has to be optimized for high-aspect ratio purpose. The KCl–NaCl salt system is taken for the molten salt technique, when this system transforms into the molten status, it acts as the solvent, K_2CO_3 and Na_2CO_3 are dissolved together with the rod-shaped Nb_2O_5 into it. The reaction then takes place at the periphery of Nb_2O_5 NRs since the dissolution amount of Nb_2O_5 is very small. Due to the mild dissolution of the Nb_2O_5 template in molten salts and the inhomogeneity of the reactants, the surface of the NRs becomes rough.

2.1.4. Sintering behaviour

Densification of the alkaline niobate based ceramics is a very challenging task. They absorb moisture from the atmosphere readily, and difficult to densify because at higher temperatures the alkalis from the material evaporates out depleting their quantity in the material. So these obstacles have left only a very little processing space in the fabrication of the high density alkaline niobate ceramic through conventional sintering route. Density of the $KNbO_3$ ceramics remains very close to the threshold when sintering under atmospheric conditions, for the closure of the open pores. Birol et al[15] has reported of 93.9% dense $KNbO_3$ which has density of 4.33 g/cm^3 on sintering at a temperature of 1035^oC in oxygen atmosphere. Kakimoto et al[16], sintered using double crucible method, in a K_2O rich atmosphere provided by extra $KNbO_3$ as sacrificial powder,at a sintering temperature of 1020$^\circ C$, touched densities of 4.49 g/cm3 (97.4%). Matsumoto et al[17] applied double stage calcination and were successful in densifying up to 4.44g/cm^3 and sintering at 1050 ◦C.

Acker et al[18] did study the microstructure and sintering of $KNbO_3$ ceramics with stoichiometric composition and also with excess-potassium and excess niobium. Stoichiometric composition $KNbO_3$ densified relatively well upto 4.36 g/cm^3. $KNbO_3$ ceramics which has potassium excess starts shrinking at a temperature of just 740^oC, but the complete densification is not achieved. Higher sintering temperature to activate sintering are required of $KNbO_3$ ceramics which has niobium in excess. Altogether, the characteristic of the stoichiometric ceramics as well as of the $KNbO_3$ ceramics with alkaline-excess or niobium excess are very similar to those described for KNN ceramics. Increase in densification didn't occur in K-excess $KNbO_3$ on changing the calcination temperatures, owing to residual K_2O for lower temperatures and at higher temperatures leading to pronounced particle coarsening. Increase in the sintering dwell time doesn't lead to increase in the density because of the formation of $K_4Nb_6O_{17}$ in addition to $KNbO_3$ due to the evaporation of potassium from the material. The key issue to achieve higher densification of the stoichiometric $KNbO_3$ material seems to be to promote the shrinkage of the material to higher levels before the start of abnormal grain growth, where the potassium oxide evaporation may also play an important role.

2.2. SPARK PLASMA SINTERING

SPS is a new technique for rapid powder densification. It has become popular with various names such as field activated sintering process (FASP), Current activated pressure assisted sintering (CAPAS), Pulsed electric current sintering (PECS), Electro-consolidation process.

It is based on the idea of electric discharge investigated in the early 1960s by Inoue et al[19] for sintering metal and ceramics where low voltage, high energy pulsed DC current passes through the powder particles and generates very high temperature between particles that causes the surface of the powder particles to melt down and surface or volume diffusion takes place as shown in fig 2.2

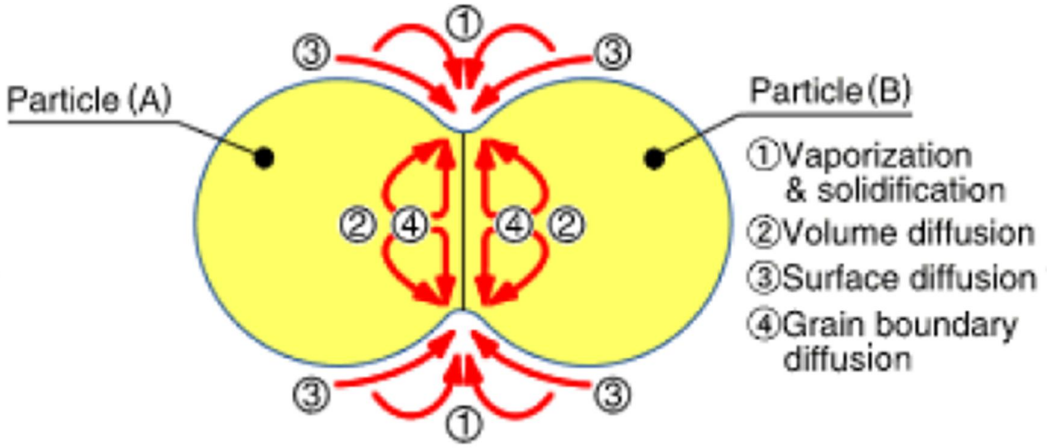

Fig. 2.2: material transfer path during sintering [20]

Pressure and current plays an important role in spark plasma sintering to reduce sintering time and increase density of the final product. SPS enables to sinter powder material at uniform heating rate to high density at relatively low temperature in shorter holding time and thus prevent extended grain growth.

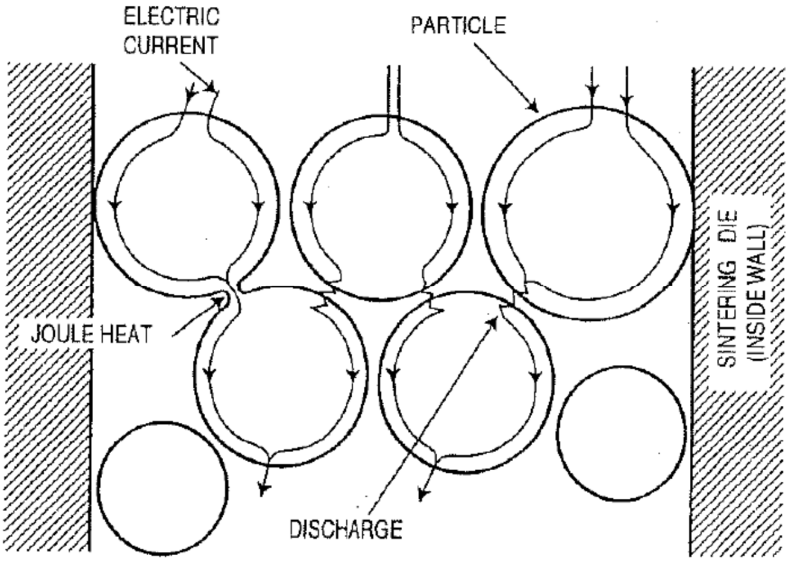

Fig.2.3: Pulsed current flow through powder particles [21]

Tokita explains that the ON-OFF DC pulse energizing method in SPS generates: (1) spark plasma, (2) spark impact pressure, (3) Joule heating, and (4) an electrical field diffusion effect. In the SPS

process the powder particle surfaces are more easily purified and activated than in conventional electrical sintering processes and material transfers at both the micro and macro levels are promoted, so a high-quality sintered compact is obtained at a lower temperature and in a shorter time than with conventional processes.

Fig 2.3 illustrates how pulse current flows through powder particles inside the SPS sintering die.

At the point when spark discharge shows up in the gap or at the point of contact between the particles of a material, a nearby high temperature-state (discharge column) is produced immediately. This reasons vaporization and softening of the powder surface of the particles in the SPS process, and the "necks" are generated at the particle area of contact. The heat is exchanged promptly from the focal point of the spark discharge column to the surface of the sphere and dispersed so that the intergranular bonding part is cooled immediately. The continuous pulse energizing technique reasons to spark discharges one after another between the particles. Even for a single particle, as the discharges are repeated the number of positions where necks are created between adjacent particles increases.

SPS was effective to sinter the alkali based compounds. Zhang et al[23] used spark plasma sintering to fabricate successfully Sodium potassium niobate ceramics with the composition of $Na_{0.5}K_{0.5}NbO_3$ when sintered at 920℃ for 5 min. They did not report any loss of sodium and potassium in the SPS sintering process, due to which the density of the $K_{0.5}Na_{0.5}NbO_3$ solid solution was raised to 4.21g/cm^3 (i.e. >93% of the theoretical density). The $Na_{0.5}K_{0.5}NbO_3$ has an orthorhombic crystal phase structure similar to that of the $NaNbO_3$ ceramics.

2.3. SUMMARY OF LITERATURE REVIEW AND SCOPE OF THE WORK

- The newly discovered $[KNbO_3]_{1-x}[Ba\ Ni_{½}\ Nb_{½}\ O_{3-\delta}\ ]_x$ (KBNNO) have attracted great attention due to the concurrence of ferroelectricity and narrow band gap ($E_g < 2$ eV).
- But not much information about the phase formation, densification, sintering behaviour and dielectric properties of this material was provided.

- Spark Plasma Sintering is a useful technique for fabrication of dense ceramics at low temperature. There is no report available on SPS of KBNNO composition.
- It is well known that microstructure and their properties may differ greatly in ceramics with the same composition fabricated with different processes, even if the same technique but different processing parameters. It will be interesting to study how the microstructure and electrical properties of KBNNO ceramics depends on different processing condition.

2.4. OBJECTIVE

To prepare phase pure highly dense $[KNbO_3]_{1-x}[Ba\ Ni_{½}\ Nb_{½}\ O_{3-\delta}\ ]_x$ (KBNNO) ceramic at a low temperature and to study its electrical properties.

To achieve the above mentioned objective we took the following steps:

(i) To study the effect of composition, calcination temperature, excess alkali on phase evolution.

(ii) To Study the densification behaviour of KBNNO powder by conventional sintering and SPS.

(iii) To study the effect of density and SPS condition on dielectric property of the KBNNO ceramics

Chapter-3

EXPERIMENTAL WORK

3.1. INTRODUCTION

In this chapter, the methods and experimental procedures used throughout this thesis are presented. The powder preparation by solid state synthesis route and the characterizing of the powder that includes the X-ray diffraction,DSC-TG, raman spectroscopy,FESEM and then the dielectric property measurements that includes permittivity and dielectric loss measurements with respect to frequency and temperature.

3.2. POWDER SYNTHESIS

3.2.1. Ball milling:-

The $[KNbO_3]_{1-x}[Ba\ Ni_{½}\ Nb_{½}\ O_{3-\delta}\ ]_x$ (KBNNO) powder was prepared by solid state mixing method via ball milling. Reagent grade of potassium carbonate [K_2CO_3 (99%)] , Niobium pentoxide [Nb_2O_5(99%)] , Barium carbonate[BaCO3(99%)] and Nickel oxide [NiO(99%)] were used as a starting material. Stoichiometric amount of powders were mixed by ball milling (zirconia ball in nylon jar) using isopropyl alcohol as the media, the mixing time was 12hrs. The mixture was then dried at 80^0C overnight in an oven. The mixture was placed in an alumina crucible which was then inserted into a furnace and heated in the temperature range of 800-1050^0C at a heating rate of 3^0C/min in the air atmosphere.

3.3. GENERAL CHARACTERIZATION

3.3.1. Thermal Analysis

3.3.1.1. Differential scanning calorimetry (DSC) and thermo gravimetry (TG)

The dried powder after ball milling was characterized by DSC and TG [NETZSCH STA (Model No. 409C) in the atmosphere of oxygen, at 10°C/min rate of heating, using α-Al_2O_3 as reference material. DSC/TG provided the information about the decomposition and phase formation behaviour of the powder.

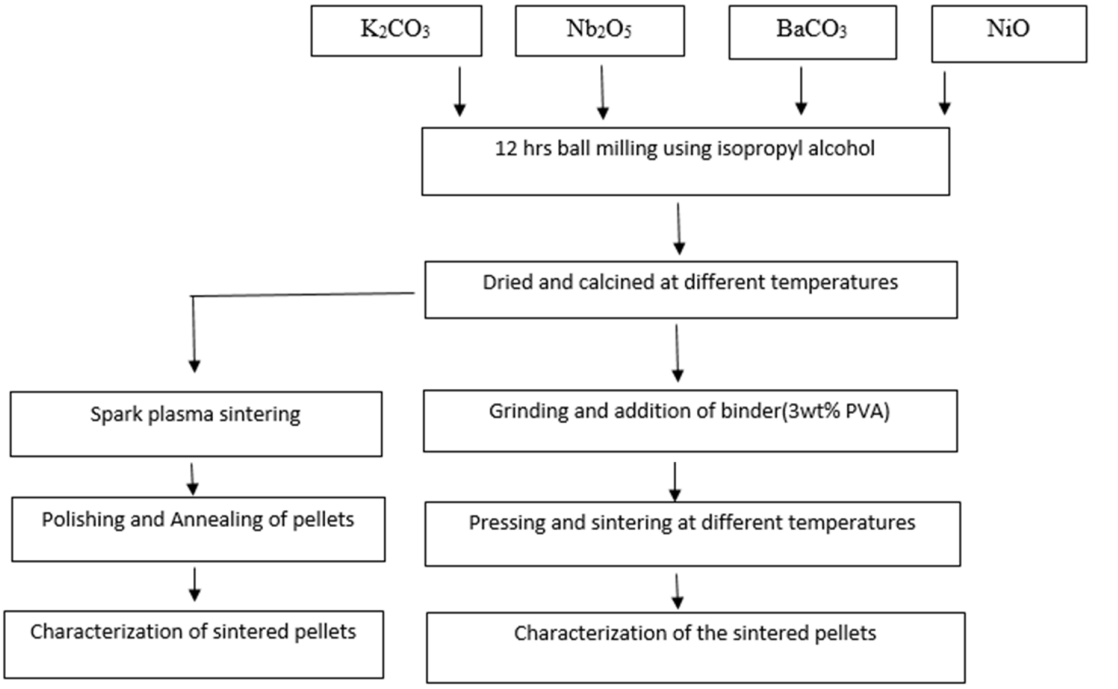

Fig. 3.1: Flow chart of the total experimental procedure followed in the synthesis of KBNNO pellets.

3.3.1.2 Densification study

Densification kinetics of the samples were investigated by dilatometer [NETZSCH Model DIL 402C]. The specimen was kept in a specimen holder at the centre of furnace of a dilatometer. The linear dimensional change i.e. specimen's shrinkage or expansion is transmitted through the pushrod (i.e. pressed onto the sample inside the furnace) into the measuring head. The samples for dilatometry were made by pressing in the form of bars having a diameter of 5mm and a lengthof 15mm. The rate of heating was maintained at 10°C/min and the measurement was carried out from the room temperature to 1090°C.in the air atmosphere.

3.3.2 Structure and Phase Analysis

3.3.2.1 X-Ray diffraction of calcined and sintered specimen

The X-ray diffraction(XRD) has proved to be a powerful and a useful tool for ananlysis of many features of fabricated potassium niobate based ferroelctric material. This non-destructive technique

measures constructively interfered monochromatic X-rays diffracted at specific angles by the crystal planes internal to the sample. A phase evolution of the calcined powder, and also of the sintered samples was studied by X-ray diffraction technique [Philips PAN Analytical, Netherland] using the Cu Kα radiation. The instrument was run at power settings of 35kV and 25mA. The samples were scanned in 2θ ranges from 15-80° with the step size of 0.05° and a scanning rate of 20°/min.

Phases present in the sample was identified with the search match facility available in the Philips X'pert highscore software.

3.3.3. Microstructure

3.3.3.1. Field emission scanning electron microscopy[FESEM]

Powder morphology, grains shape and size were observed by FESEM [Nova Nano SEM 450] which was equipped with an energy dispersive X-Ray spectrometer(EDX). The samples were coated with gold for FESEM using a sputter coater for time span of 4mins.

3.3.4. Raman Spectra Analysis

The room temperature spectroscopic measurement was performed in the frequency range of 50cm^{-1} to 1400cm^{-1} using an Raman spectroscope (STR500, Cornes Technologies, formerly known as Seki Technotron) to evaluate the samples. 514.5nm Ar+ ion green laser was used with 50 mW power. The Raman signals were taken over variable exposure time with different number of data acquisition, using 1200 grating size and 50X objective lens of the spectrometer. It depends on inelastic scattering or raman scattering of the monochromatic light usually from a laser in the visible, near infra-red and near ultra-violet range. The Phonons or other excitations in the material or emitted by the laser light, that results in the energy of the laser photons to shift up or down are measured. This shift in energy provides information about the different phonon modes in the system. Raman scattering is used to study the phase formation, phase transition, and B-site ordering/disordering of normal ferroelectrics.

3.3.5. Preparation of Bulk Sample

3.3.5.1. By conventional sintering

For the preparation of bulk sample, calcined powders were mixed with 3wt% PVA(Poly Vinyl Alcohol) solution with the help of mortar and pestle and dried. The dried powders were pressed into cylindrical pellets (12mm diameter and 1-2 mm thickness) at 4tonn pressure in a hydraulic press [Carver Inc. USA] with the holding time of 120secs. The pressed green compacts were kept inside an alumina container with sacrificial KBNNO powder around the pellets to prevent the removal of potassium from the pellets at higher temperatures, and the container was covered with an alumina plate and were sintered in air at a heating rate of 3°C/min in the temperature range of 1050-1150 °C for 2hrs with a binder burnout at 650°C for 1hr in a conventional furnace.

3.3.5.2. By Spark plasma sintering

Spark Plasma Sintering is a new method which takes just a few minutes to complete the sintering process in comparison to the conventional sintering that takes hours or even days for the same. Since time for coarsening and grain growth were given, no grain growth occurs, and thus high densities could be reached in a very short time. Control over grain growth improves the properties of the material.

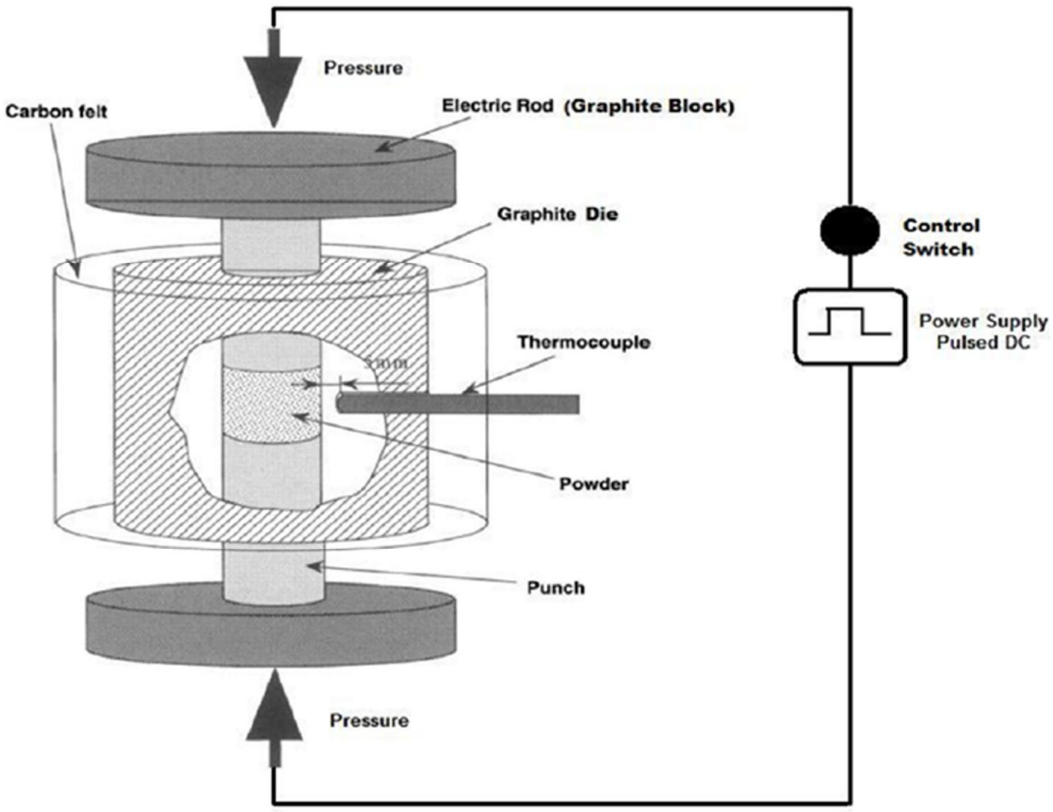

Fig. 3.2: The schematic diagram for the spark plasma sintering process.[20]

Around 3 gm of doubly calcined KBNNO powder sample was taken in a cylindrical graphite die lined with graphite sheets, which facilitates the easy removal of the sintered compact. The chiller-compressor and the machine were switched ON. The die containing the powder sample was placed in the SPS chamber. The high sintering can be done by two modes (1)pulsed current mode (2) DC current mode. In the pulsed current mode the t_{on} was set on 50ms and t_{off} at 5ms, the samples were heated at a rate of 100°C/min between 1000°C - 1100°Cand holding time was varied from 5min-15min. The cooling rate was given to be 25°C/min. A force of 11kN was applied simultaneously over the sample. In the DC current mode only the pulsed current is replaced by a non-fluctuating DC current other conditions remaining same. The graphite sheets were removed from over the sintered pellets, and the pellets were polished. The polished pellets were given for annealing in a conventional furnace at 820°C for 6 hrs.

3.3.6 Density Measurements

The bulk density of the samples was measured by Archimedes principles. The formula for the calculation of bulk density is as follows

$$Bulk\ density = \frac{W_d}{W_s - W_{su}} X\ Density_{liquid}$$

$$Relative\ density = \frac{Bulk\ density}{Theoritical\ density} X\ 100$$

Where W_d, W_s and W_{su} are the dry weight, soaked weight and suspended weight of the sample, respectively. The liquid used for calcination was kerosene of density 0.81 g/cc.

3.3.7 Dielectric Measurements

For electrical measurements both the surfaces of the pellets were painted uniformly with silver conductive paste (Alfa Aesar) and cured 500°C for half an hour. Thus, a pellet with two parallel electrodes acts as a single layer capacitor.

The dielectric constant or relative permittivity (ε_r) is defined as the ratio of the permittivity of the material to the permittivity of free space. The dissipation factor is defined as the tangent of the loss angle (tan δ) was measure of the amount of the electrical energy which is lost through conduction when a voltage is applied across the piezoelectric element. The dielectric constant (ε_r) and dielectric loss factor (tan δ) was measured using Solatron SI 1260 Impedance/ Gain-phase analyser and HIOKI 3532-50 LCR Hitester. Measurements are carried out in the frequency range of 100 Hz to 1MHz. Dielectric behaviour has also been studied as a function of temperature with the temperature ranging from room temperature to 550°C depending on the composition. The samples were placed in between two platinum sheets each of which is connected to a platinum wire. The whole arrangement was covered with an alumina tube. A small force was applied using a spring to ensure good contact

with the sample electrodes. The dielectric measurement was carried out in a Carbolite furnace at a heating rate of 5°C/min.

The relative permittivity (ε_r) is calculated from the measured values of capacitance and physical dimension of the specimen. The relations are expressed as:

$$C = \frac{\varepsilon_0 \varepsilon_r A}{t}$$

Where ε_r is the relative permittivity of the piezoelectric material, ε_0 is the relative permittivity of free space (8.854 x 10^{-12} F/m), t is the distance between electrodes (m), A is the area of the electrodes (m^2).

In an alternating electric field the dielectric permittivity or relative permittivity is a complex quantity and can be written as

$$\varepsilon_r^* = \varepsilon' + \varepsilon''$$

Where ε' is the real part of the dielectric permittivity and ε'' is the imaginary part of permittivity and related to the energy loss in the system.

When the dielectric is subjected to the ac voltage, the electrical energy is absorbed by the material and is dissipated in the form of heat. The dissipation is called dielectric loss. In this case current leads the voltage by (90-δ), where δ is called the loss angle, and tanδ is the electrical loss, as shown in the figure 3.3.

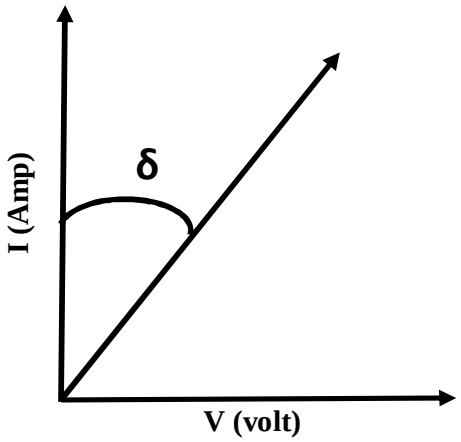

Fig. 3.3: Phase diagram between current and voltage.

The loss tangent can be expressed as

$$tan\delta = \frac{\varepsilon''}{\varepsilon'}$$

Curie temperature (Tc): It is the temperature above which the spontaneous polarization (Ps) of the ferroelectric materials vanishes and it goes to paraelectric state.

Chapter-4

RESULTS AND DISCUSSION

4.1 THERMAL ANALYSIS AND PHASE EVOLUTION

Figure 4.1 shows the thermal analysis of un-calcined oxide mixture obtained after ball milling. According to the TGA plot, an overall weight loss of 17% is observed. The total weight loss can be divided in two steps. In the first step (room temperature – 120^{o}C), minor weight loss of about ~6% is observed that could be due to removal of absorbed moisture and isopropyl alcohol. In the second step, the sample shows a major weight loss of about 11% in the temperature range 610^{o}C – 900^{o}C. This 11% weight loss is also matching with the wt. loss due to decomposition of K_2CO_3 and $BaCO_3$ present in oxide mixture. Broad peaks can be observed in the corresponding DSC curve around 700^{o}C and 900^{o}C. These peaks could be attributed to the decomposition of carbonates and crystallization of perovskite phase.

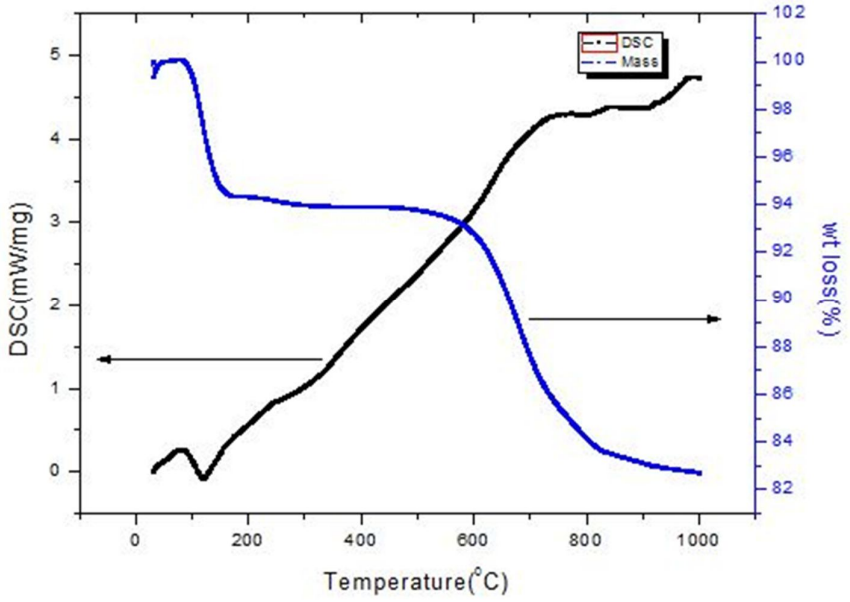

Fig. 4.1: DSC-TG curve for KBNNO-0.1 uncalcined powder after 12h milling.

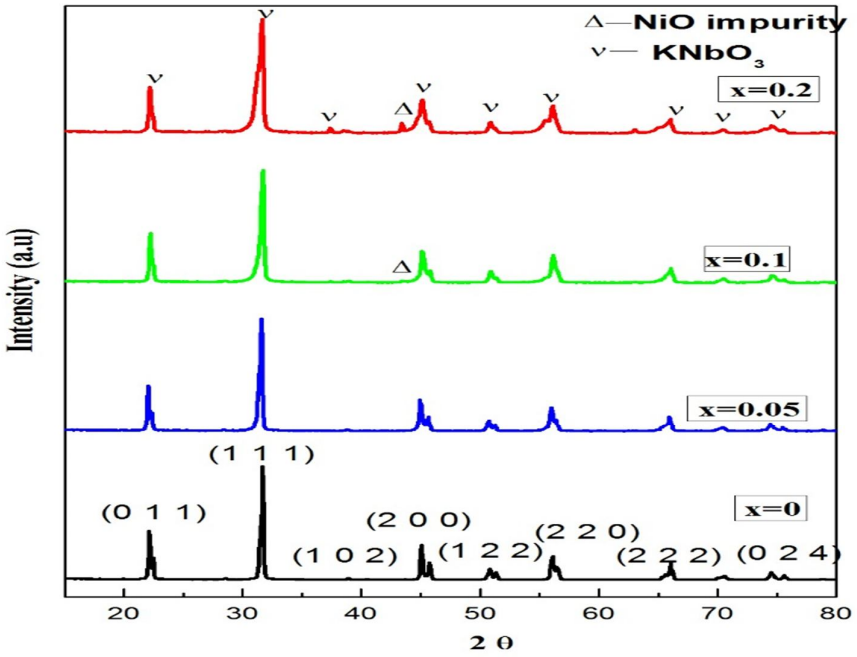

Fig. 4.2: XRD patterns of the (1-x) KN- x BNNO powder with x = 0, 0.05 ,0.1, 0.2.

Fig.4.2 shows the X-ray diffraction patterns of the KBNNO powder calcined at 900°C. All the compositions possess a pure perovskite structure. For x= 0.1 and 0.2, a small amount of NiO secondary phase is observed. Grinberg et.al. [10] synthesized the powder by calcining at 900°C/12h. In our case, powder was calcined at 900°C/6h twice and with an intermediate grinding. Formation of pure perovskite structure suggests that the Ba and Ni have diffused into the lattice site of $KNbO_3$ to form homogeneous solid solution. Moreover, it is clear that the position of diffraction peaks of the KBNNO has shifted to lower angle with increase in BNNO content indicating increase of the lattice parameters of the ceramics. It is due to the distortion of crystal lattice induced by the substitution of Nb^{5+} (0.64A°) by larger Ni^{2+} (0.69A°).The KN and KBNNO ceramics exhibit orthorhombic phase and matching with the JCPDS No. 71-0946 having space group Amm2. Lattice parameters for KN and KN-BNNO were calculated and shown in table 4.1 which closely matches with the literatures

value[11]. It is clear from the table that lattice parameter is increasing BNNO addition. For 0.2 BNNO addition lattice parameter decreases that may be due to the higher amount of NiO impurity.

It was also observed that the addition of 2-5 wt.% excess potassium reduces the impurity NiO content in the final ceramics. Calcination temperature above 800^{o}C produces phase purity.

Table: 4.1 Lattice parameters of different KN-BNNO sample

	a (Å)	b (Å)	c (Å)	Volume (Å)^3
KN(x=0)	3.9689(3)	5.6899(7)	5.7077(4)	128.9
x=0.05	3.9753(3)	5.6977(5)	5.7104(2)	129.44
x=0.1	3.9758(11)	5.6971(18)	5.7091(2)	129.31
x=0.2	3.9733(3)	5.6807(8)	5.7088(6)	128.86

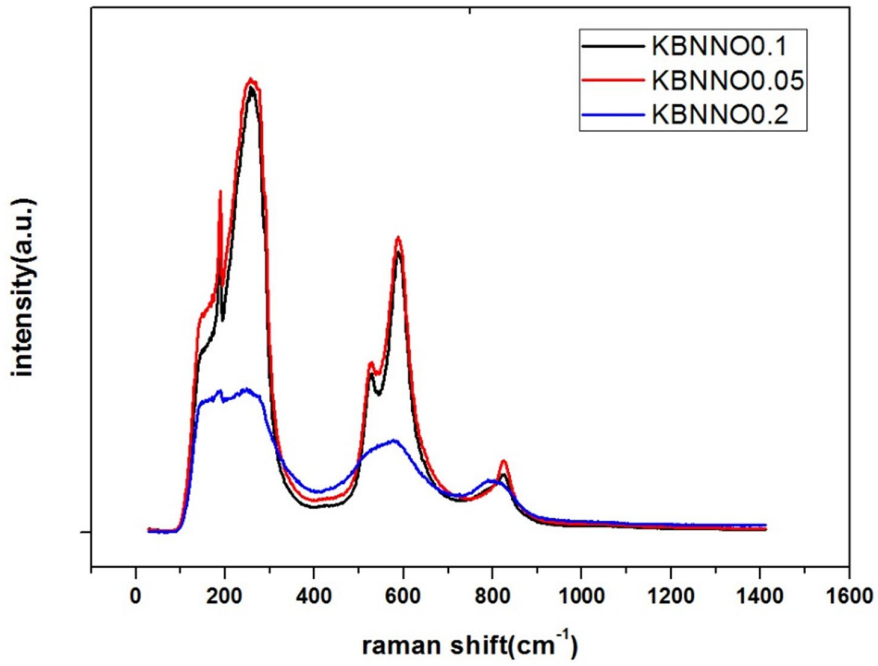

Fig. 4.3: Raman spectroscopy of different KBNNO powders

Raman spectroscopy is also useful to analyze the structure and the phase evolution of KBNNO samples besides XRD analysis. Raman spectroscopy (Fig. 4.3) shows a resonance depth at 197 cm^{-1} and a peak at 825cm^{-1} for x=0.1 and x=0.05 compositions; these have been identified as signatures of ferroelectricity in $KNbO_3$- based solid solutions [10]. Peaks become broader for x=0.2 composition

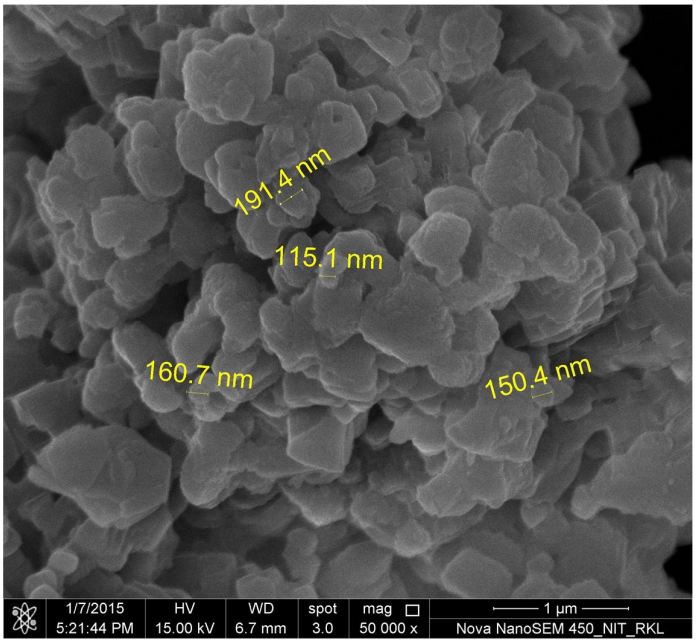

Fig.4.4: The powder morphology of the double calcined KBNNO-0.1 powder

Fig4.4 shows the FESEM micrograph of KBNNO-0.1 powders calcined at 900°C. The synthesized powder has agglomeration; the size of agglomerates is in the range of 0.1–0.7 µm.

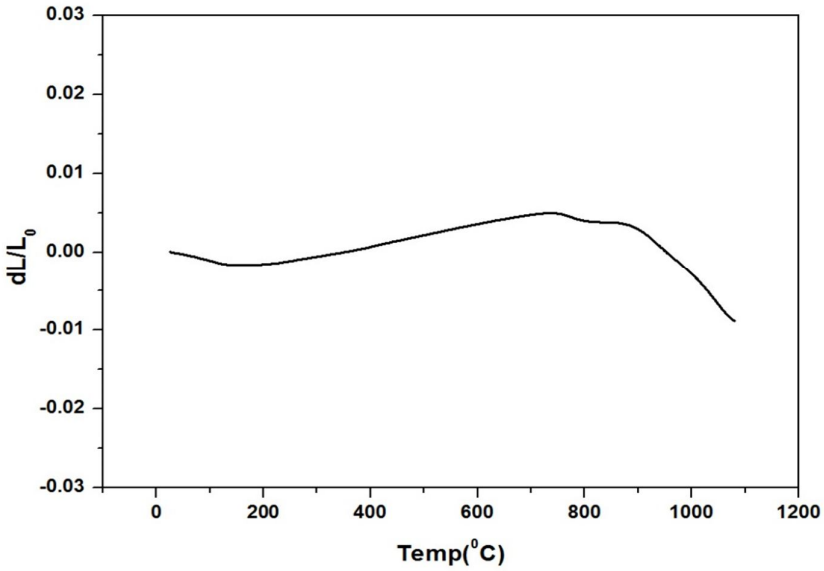

Fig. 4.5: Dilatometry of the KBNNO-0.1 calcined sample

4.2. DENSIFICATION BEHAVIOUR

Fig 4.5 shows the linear shrinkage as a function of temperature for KBNNO-0.1 sample. Linear shrinkage behavior was studied upto 1080^{o}C. It is observed that the linear shrinkage is around 1.3% in the temperature range of 800^{o}C to 1080^{o}C. Further studies are required to understand the non-isothermal linear shrinkage behavior of KBNNO sample

4.2.1. Conventional Sintering

Fig 4.6 shows the variation of density with temperature of KBNNO-0.1 ceramic. The bulk density of the KBNNO pellets increases with the increase in sintering temperature. Volume shrinkage was also increased with the increase in the sintering temperature. For all the samples dwelling time at peak temperature was 2h. Further increase of sintering temperature from 1120^{o}C to 1140^{o}C resulted melting of the sample. The dwelling time was varied for 1120^{o}C sintered sample. Maximum density was achieved for 2h dwelling time sample. It is to be mentioned that with increase in dwelling time density decreases and deformation of the sample observed. All the pellets were sintered in covered

alumina crucible surrounded by sacrificial powder of the same composition to inhibit volatilization of potassium. We could achieve only 83% of the true density (measured true density for KBNNO-0.1 is 4.62 gm/cc) for KBNNO-0.1 sample.

The pellets sintered by conventional sintering didn't sinter or densify well, it densified only upto 83% of the theoretical density. So the powder were tried to sinter by spark plasma sintering

The pellet fired at 1120/2h showed the highest bulk density and lowest apparent porosity. On firing the pellets at 1140/2h, the pellets melted and got stuck to the base plate.

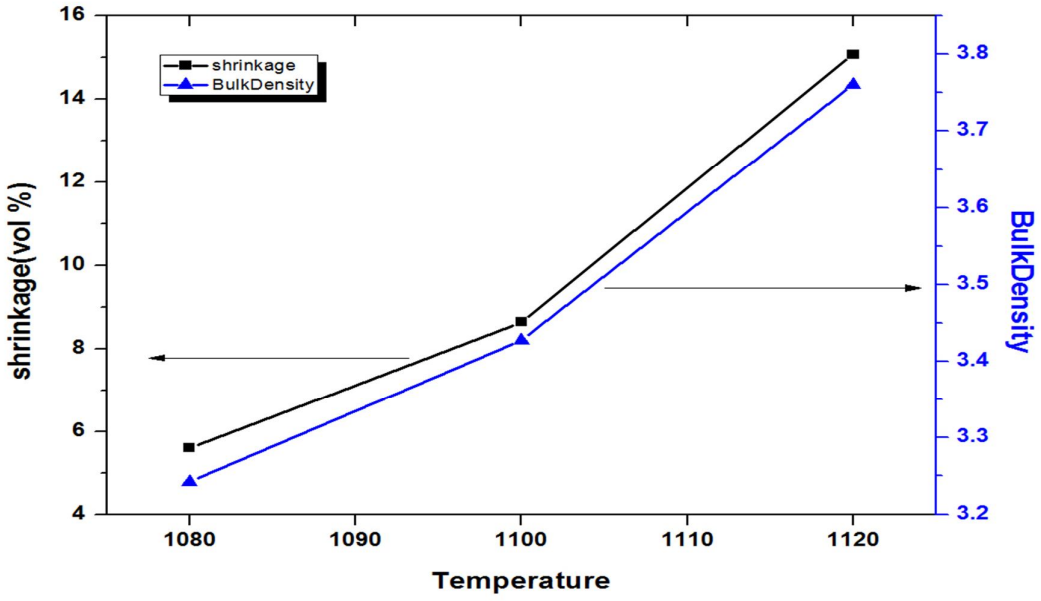

Fig. 4.6: Bulk density and volume shrinkage with respect to temperature of the sintered pellets

4.2.1.1 Microstructure of Conventional Sintered Sample

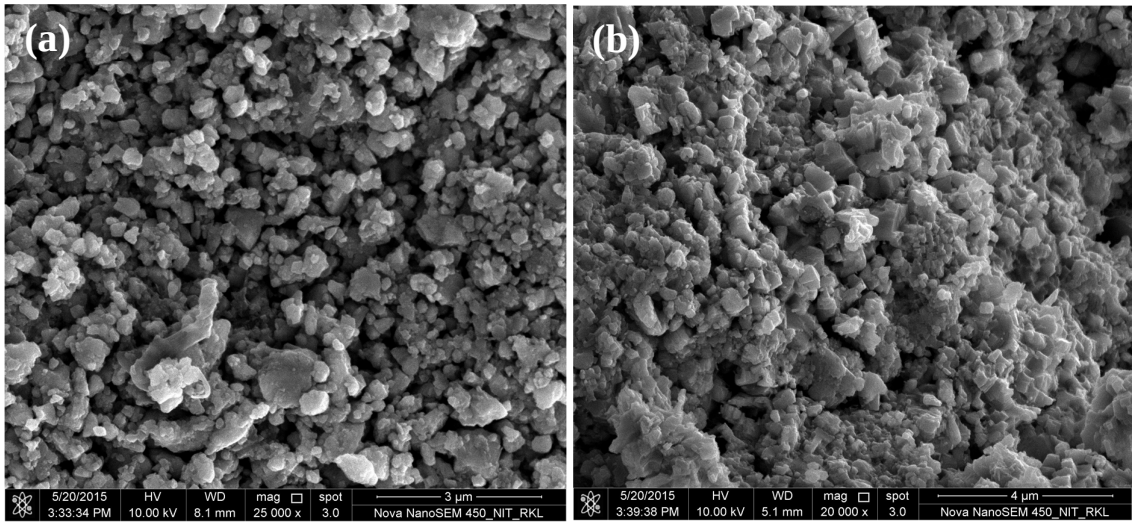

Fig.4.7: Microstructures of (a) surface and (b) fracture of the conventionally sintered sample sintered 1120/2h

4.2.2. Spark plasma sintering of KBNNO

In earlier section we observe the difficulty of fabricating high-density KBNNO ceramics because of the high volatility of the potassium during the sintering process. Recently, spark plasma sintering (SPS) has been increasingly used instead of conventional sintering or hot pressing because of its advantages of a rapid heating rate and short soaking time. Here SPS was used to prepare highly dense KBNNO ceramics. SPS was carried out at different temperatures in the range of 800-1075^{o}C for 10-15 minutes.

It was found that the SPS sample changed to a dark gray color from the greenish white-colored powder, but there was no difference in the XRD patterns of both samples, provided that the surface of the SPS sample was polished away sufficiently. The SPS sample became dark gray in color because of oxygen deficiency in its crystal lattices, which was caused by the reduced atmosphere of SPS. Fig4.8. shows the TG plot of grounded unannealed sps1050 pellets. It was observed that a small

weight gain was observed at around 820^{o}C which could be due to oxygen intake of the samples. A weight loss was observed beyond 970^{o}C which could be due to alkali evaporation.

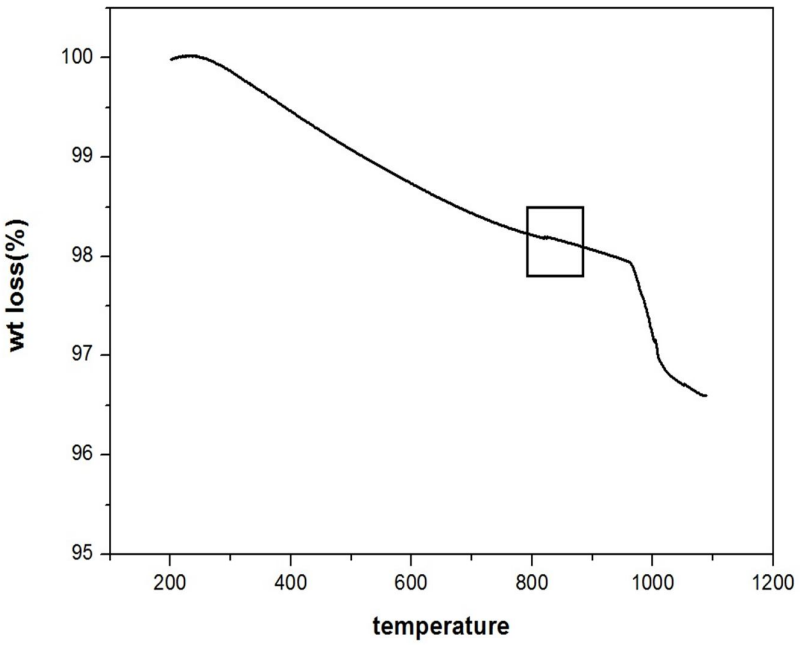

Fig. 4.8: TG plot of unannealed sps1050 sample

4.2.2.1. Annealing

The annealing treatment in the air (820^{o}C/6h) changed the color from dark gray to greenish white, probably because the oxygen deficiency was supplemented during the annealing process. Annealing at higher temperature produces needle shape K_2CO_3 (Fig 4.9) which corroborates the weight loss around 970^{o}C.

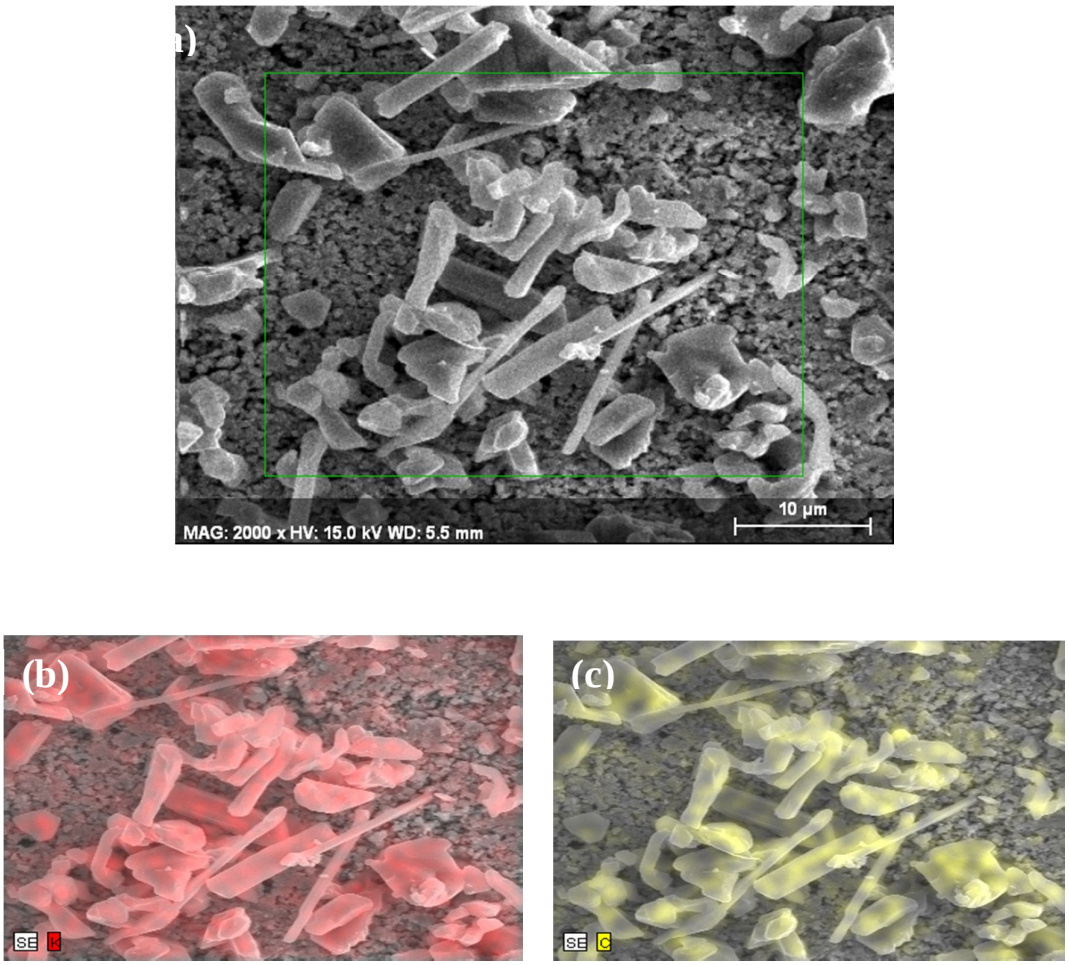

Fig. 4.9: (a)Surface FESEM image and (b) and (c) showing mapping of potassium and carbon came to the surface of the SPS pellet sample annealed at 950°C

Table 4.2 shows the change in sintered density of the SPS sample as a function of sintering temperature. When the temperature was increased to 1050^{o}C, bulk density increased with temperature and reached 4.46 g/cm^{3}, which was 96.5% of the true density. In contrast, the conventional sintering could produce only 83% of true density at 1120^{o}C. In case of KBNNO-0.2, we could achieve 97% of the true density (measured true density for KBNNO-0.2 is 4.72 gm/cc) for KBNNO-0.2 sample. The density of KBNNO samples improves slightly for DC mode SPS.

Table 4.2: shows the bulk density of all the spark plasma sintered pellets.

Sample	Sintering temperature and time (in minute)	Bulk Density
0.1 KBNNO (pulsed)	800/5min	Didn't sinter
	900/5min	Didn't sinter
	950/15min	Didn't sinter
	1050/10min	4.465
	1075/10min	4.322
0.1 KBNNO (DC)	1075/15min	4.571
0.2 KBNNO (pulsed)	1075/15min	4.563
0.2 KBNNO (DC)	1100/15min	4.616

4.2.2.2. Microstructure

Figure 4.10(a)-(b) shows FESEM micrographs of the KBNNO-0.1 ceramics SPS at 1050^{o}C for 10 min. The micrograph of the fractured surface shows that this sample was very dense, and almost no visible pores could be found in it. Moreover, the same composition when sintered in DC mode, a fibrous microstructure evolved [Fig – (c) and (d)].

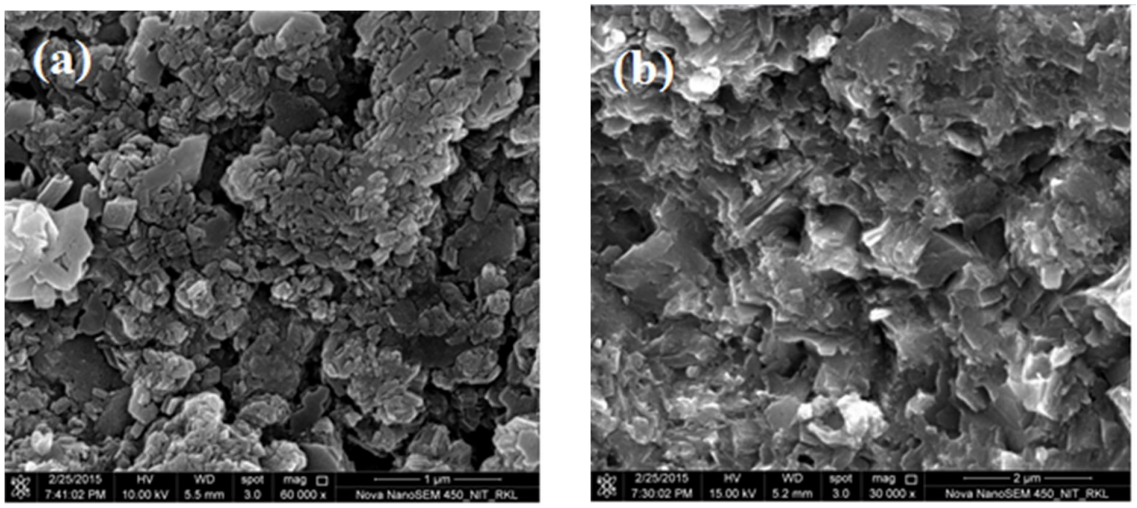

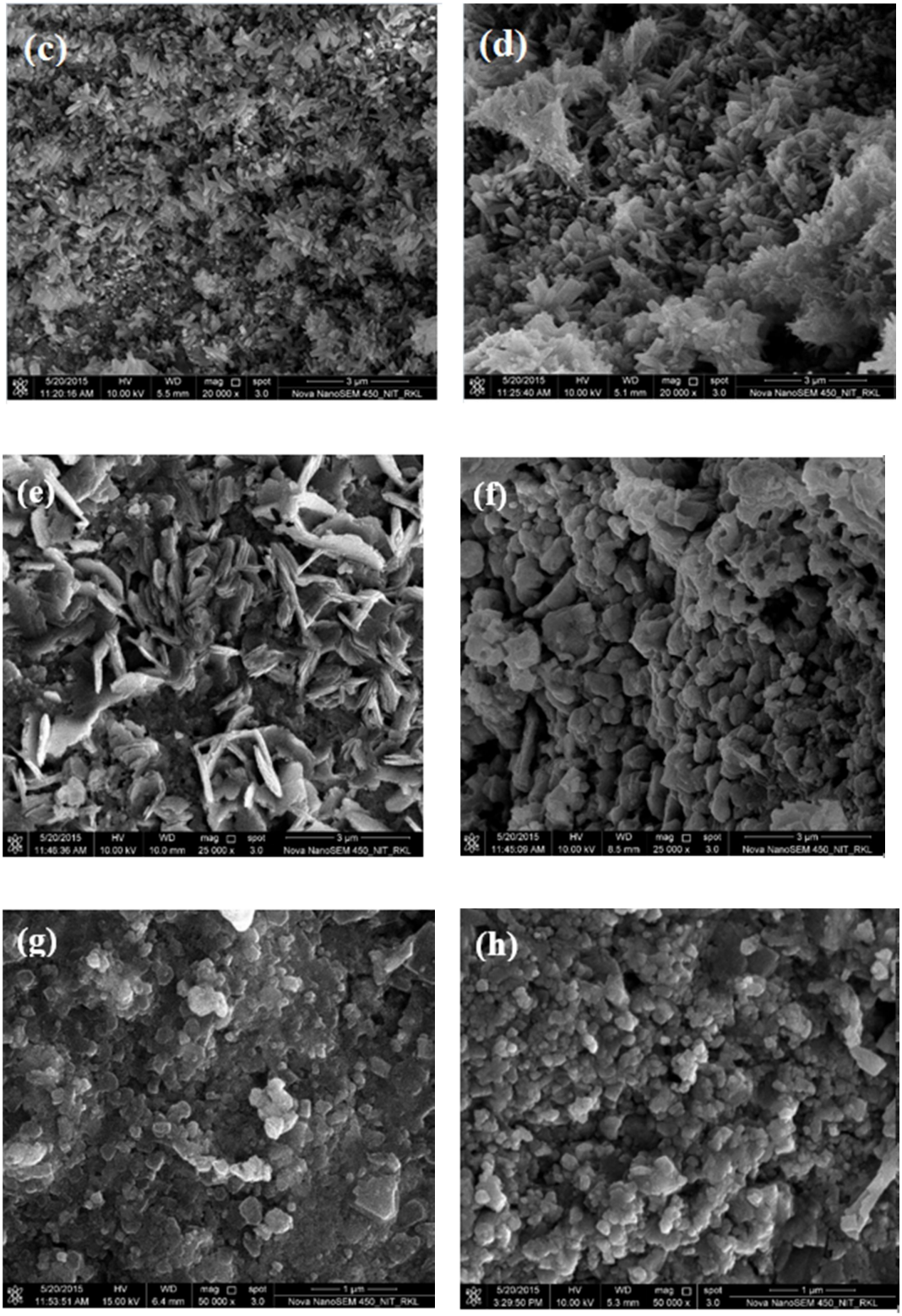

Fig. 4.10: FESEM images of as-fired surfaces of KBNNO 0.1 (a) pulsed, (c) DC, KBNNO 0.2 (e) pulsed and (g) DC. FESEM images of fracture surfaces of KBNNO 0.1 (b) pulsed, (d) DC, KBNNO 0.2 (f) pulsed and (h) DC.

4.3. DIELECTRIC PROPERTY MEASUREMENT

4.3.1. Variation of Dielectric property with respect to Frequency

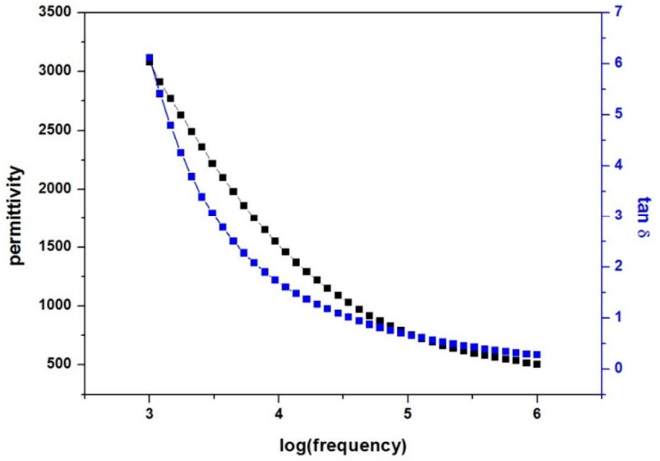

Fig. 4.11: Variation of permittivity and dielectric loss with frequency of conventional sintered KBNNO-0.1samples sintered at 1120°C.

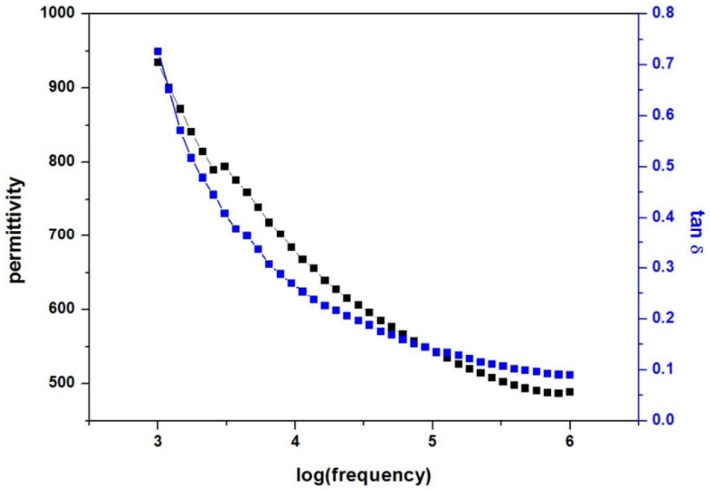

Fig. 4.12: Variation of permittivity and dielectric loss with frequency of spark plasma sintered KBNNO-0.1 sample

Fig. 4.11 and 4.12 shows the frequency dependent dielectric behavior of CS and SPS1050 samples. The permittivity for CS samples at low frequencies is higher than that of SPS samples. Incidentally, the enhancement of dielectric constant at low frequency for CS (in contrast to SPS) is also associated

with a high dielectric loss. Also the dielectric loss tends to increase without showing a peak at low frequencies. This is a signature of Maxwell–Wagner type relaxation, which is the consequence of charge accumulation at the discontinuities/grain boundaries within the dielectrics. Low dielectric loss in SPS sample may be attributed to higher relative density (low porosity) of SPS ceramics.

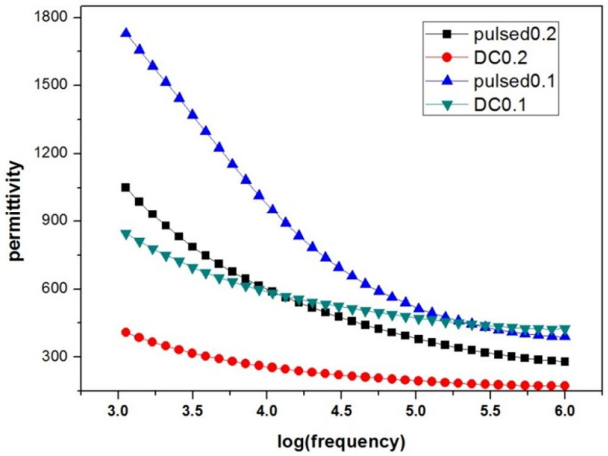

Fig. 4.13: Variation of permittivity with respect to frequency of spark plasma sintered KBNNO-0.1 and KBNNO-0.2 under Pulsed DC and DC mode

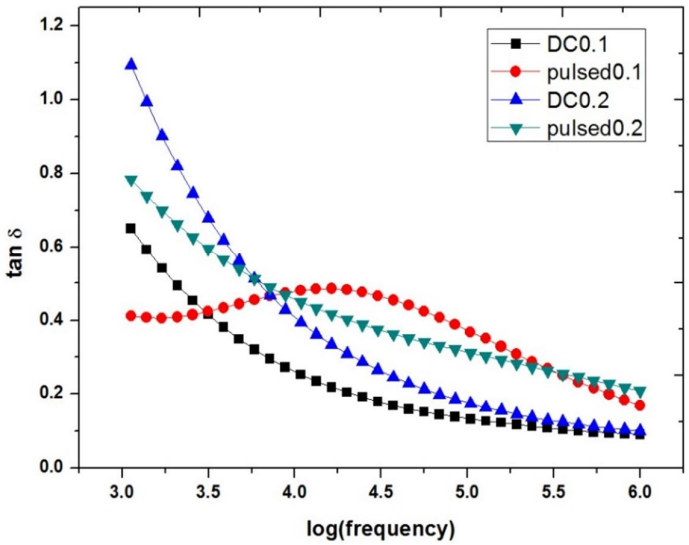

Fig. 4.14: Plot showing the dielectric loss Vs frequency of spark plasma sintered KBNNO-0.1 and KBNNO-0.2 under Pulsed DC and DC mode

Fig. 4.13 and Fig 4.14 shows the frequency dependent dielectric behavior of KBNNO-0.1 and KBNNO-0.2 SPS sintered in pulsed DC and pure DC mode. However, they have comparable density but very different dielectric property. DC mode sample has lower permittivity compared to the pulsed mode. Further studies are required to understand this behavior.

4.3.2. Dependency of Dielectric Property with respect to Temperature

(1) Conventionally sintered pellet at 1120/2h

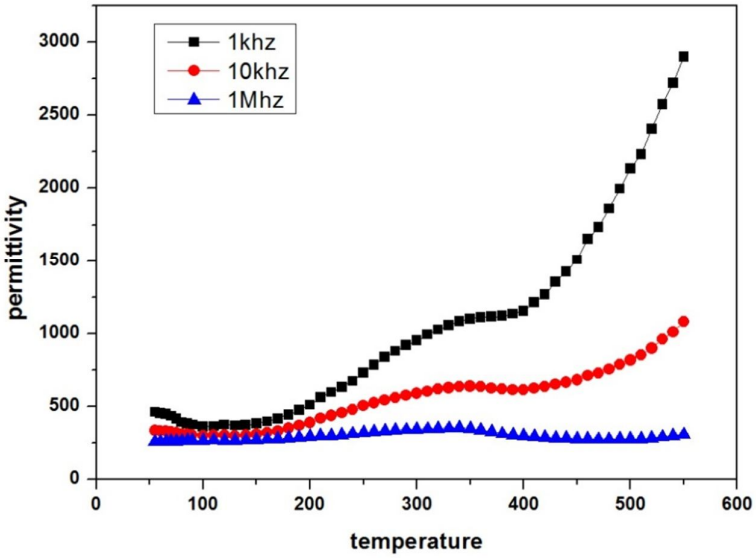

Fig. 4.15: Plot showing the permittivity with respect to temperature at different frequency of the conventionally sintered KBNNO-0.1sample

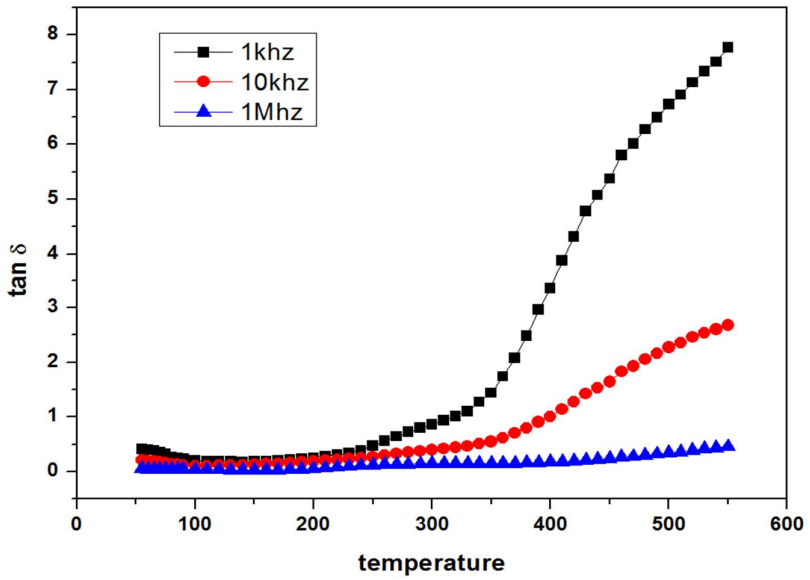

Fig. 4.16: Plot showing dielectric loss with respect to temperature of the conventional sintered sample

(2) 0.1 KBNNO pulsed SPS-1050

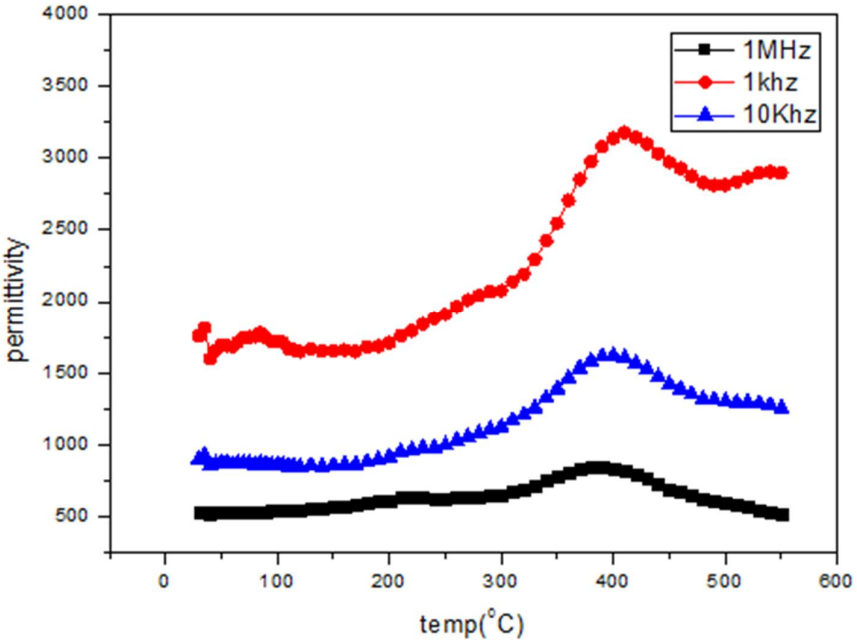

Fig. 4.17: Plot showing the change in permittivity with respect to temperature of the spark plasma sintered sample

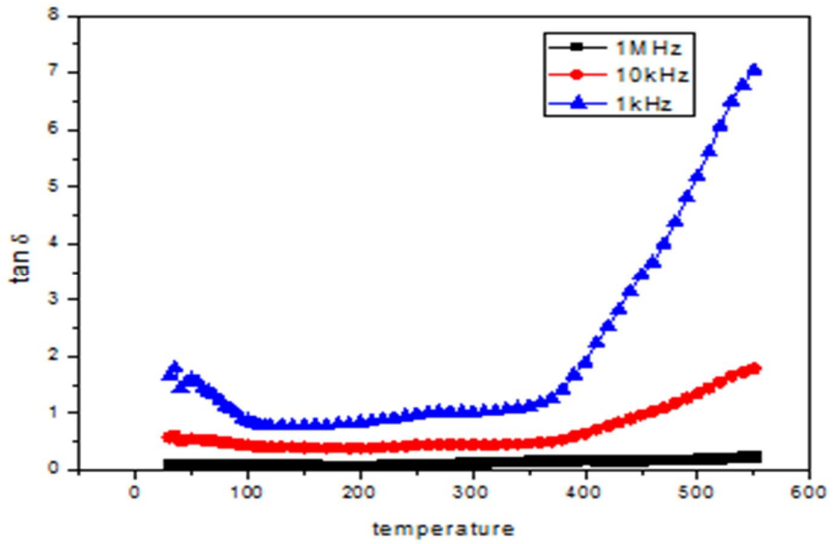

Fig. 4.18: Dielectric loss with respect to temperature at different frequencies of the sps sintered sample in pulsed mode.

Fig.4.15-4.18 shows the temperature dependence of dielectric permittivity and dissipation factor of KBNNO-0.1 for CS and SPS1050 sample. The results indicate thermally activated dissipation process. The CS sample exhibited an inflection point at 370^{o}C which may be due to orthorhombic to cubic phase transition. For SPS sample peak was observed at 390^{o}C. The difference in peak temperature may be attributed to compositional inhomogeneity or difference. Dielectric loss of the sintered sample increases significantly beyond 350^{o}C

CONCLUSIONS

KN-BNNO solid solution was prepared successfully by conventional solid state mixing method via ball milling. Phase pure KBNNO-0.1 powder could be prepared at 900^{o}C. With increase in BNNO concentration NiO secondary peak was appeared in the calcined powder. With incorporation of BNNO in KN crystal structure changes and lattice parameter increases. KBNNO solid solution contains orthorhombic phase at room temperature. Raman spectroscopy shows a resonance depth at 197 cm^{-1} and a peak at 825cm^{-1} for x=0.1 and x=0.05 compositions; these have been identified as signatures of ferroelectricity in $KNbO_3$ based solid solutions. Peaks become broader for x=0.2 composition indicating transformation to more symmetric structure. By conventional sintering only 83% of true density can be achieved at 1120^{o}C/2h. Spark plasma sintering is very useful to get highly dense (96% of true density) sample at 1050^{o}C/10 min. It is observed that the microstructure and dielectric property of SPS sample significantly depends on the SPS condition. In addition, DC mode SPS sample has higher density compared to pulsed DC mode which resulted in the lower dielectric loss of the DC mode SPS sample compared to that of the pulsed mode. The curie temperature of the KBNNO-0.1 sample sintered through SPS in Pulsed mode was found to be 390^{0}C.

REFERENCES

1. A.J. Moulson and J.M.Herbert, Electroceramics-Materials-properties-applications Chapman and Hall, London, p.18, 52,277 (1990).
2. Synthesis and Characterization of Zr and Ca modified $BaTiO_3$ Ferroelectric Ceramics" PhD Thesis Ganesh Kumar Sahoo, NIT Rourkela, 2015
3. T. Choi, S. Lee, Y. J. Choi, V. Kiryukhin, and S. W. Cheong, Science 324, 63 (2009).
4. S. Y. Yang, L. W. Martin, S. J. Byrnes, T. E. Conry, S. R. Basu, D. Paran,L. Reichertz, J. Ihlefeld, C. Adamo, A. Melville, Y. H. Chu, C. H. Yang, J.L. Musfeldt, D. G. Schlom, J. W. Ager III, and R. Ramesh, Appl. Phys.Lett. 95, 062909 (2009).
5. Zhang, G.H. New high Tc multiferroics $KBiFe_2O_5$ with narrow band gap and promising photovoltaic effect. Sci. Rep. 3, 1265; (2013). DOI:10.1038/srep01265
6. Choi, W. S. *et al.* Wide bandgap tunability in complex transition metal oxides by site-specific substitution. *Nat. Commun*. 3:689, (2012) doi: 10.1038/ncomms1690
7. Xiaoning Li, et al. J. Mater. Chem. A, 2,13366, 2014.
8. B. T. Matthias, J. P. Remeika, Phys. Rev., 82, 727, (1951)
9. G. Shirane, H. Danner A. Pavlovic, R. Pepinsky, Phys. Rev., 93, 672, (1954)
10. Ilya Grinberg et al., Nature 503, 509 (2013) doi:10.1038/nature12622.
11. Wang, D.; Kako, T.; Ye, J. J. Am. Chem. Soc., 130, 2724−2725, (2008)., G. Naresh and T. K. Mandal.ACS Appl. Mater. Interfaces, 6, 21000−21010, (2014)
12. W. Zhou, H. Deng, P. Yang, and J. Chu, Appl. Phys. Lett. 105, 111904 (2014)
13. Li-Qian Cheng, Synthesis of highly piezoelectric lead-free (K, Na)NbO_3 one dimensional perovskite nanostructures, Chem. Commun., **49**, 4003, (2013).
14. G. K. L. Goh ,C. G. Levi , J. H. Choi , F. F. Lange , J. Cryst. Growth 286 , 457, (2006).
15. Birol H, Damjanovic D, Setter N. Preparation and characterization of $KNbO_3$ ceramics. J Am Ceram Soc;88:1754–9, (2005)

16. Kakimoto K-I, Masuda I, Ohsato H. Lead-free $KNbO_3$ piezoceramics synthesized by pressureless sintering. J Eur Ceram Soc;**25**:2719–22, (2005)
17. Matsumoto K, Hiruma Y, Nagata H, Takenaka T. Piezoelectric properties of $KNbO_3$ ceramics prepared by ordinary sintering. Ferroelectrics;358:169–74, (2007)
18. Jerome Acker, Journal of the European Ceramic Society 33, 2127–2139, (2013)
19. Inoue, K. Electric Discharge Sintering. U.S. Patent 3,241,956, filed October 29, 1963,and issued March 22, 1966
20. M. Suárez, Challenges and Opportunities for Spark Plasma Sintering: A Key Technology for a New Generation of Materials, INTECH, 2013, http://dx.doi.org/10.5772/53706
21. M.tokita, mechanism of spark plasma sintering, xa.yimg.com/.../SUMITOMO%20REVIEW-Spark-Plasma-Sintering.pdf.
22. Bo-Ping Zhang et al., Materials Science Forum Vols. 475-479 (2005) pp. 1165-1168